The Radio Sky

Lecture 14

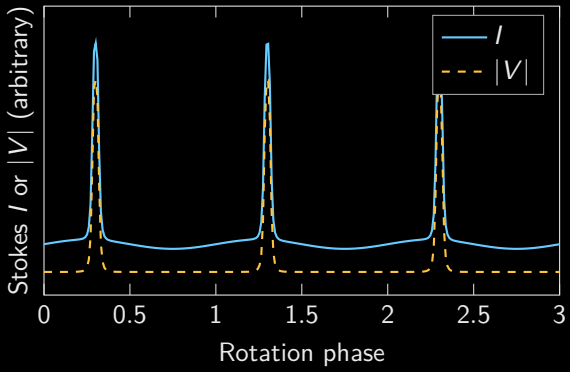
Yogesh Wadadekar

National Centre for Radio Astrophysics (NCRA-TIFR), Pune

PHY-236.3



Ultracool dwarfs: auroral pulsars



Schematic light curve: quiescent emission plus periodic, nearly fully circularly polarized pulses.

- Late M, L and T dwarfs show pulses at the rotation period (hours), with $\sim 100\%$ circular polarization [Hallinan et al. 2008, doi:10.1086/590360].
- Interpretation (L9): Jupiter-like auroral ECM, not Solar-like flaring.
- GHz ECM from T dwarfs implies kG fields in objects of planetary-like mass scale [Kao et al. 2016, doi:10.3847/0004-637X/818/1/24].
- They bridge stars and planets.

Why search for radio emission from exoplanets?

- ECM emission is the only known direct probe of an exoplanet's magnetic field: $\nu_{\max} \Rightarrow B_{\max}$, as for Jupiter (Lecture 9).
- Field strength constrains interior dynamo models; scaling laws based on convective energy flux predict tens of gauss for massive planets [Christensen et al. 2009, doi:10.1038/nature07626].
- Magnetospheres affect atmospheric escape and habitability.
- Rotation period from periodicity; orbital phase dependence would tie emission to the planet.

Predicted power: the radiometric Bode's law

In the Solar System, auroral radio power scales roughly linearly with the solar-wind (kinetic or magnetic) power intercepted by the magnetosphere. Extrapolated to hot Jupiters in dense stellar winds, this predicts 10^3–10^5 times Jupiter's power [Farrell et al. 1999, doi:10.1029/1998JE900050; Zarka 2007, doi:10.1016/j.pss.2006.05.045]. Empirical scaling over orders of magnitude.

Five limitations of exoplanet radio searches

1. Frequency cutoff. Ground-based detection needs $B_{\max} \gtrsim 3.6\,\mathrm{G}$ (see above); ionospheric distortion makes 10–30 MHz hard even above that.
2. Flux. Even with 10^3–10^5 amplification, predicted bursts are ∼mJy at tens of pc: at the limit of LOFAR/NenuFAR-class arrays.
3. Beaming and duty cycle. A hollow cone illuminates Earth only for some geometries and phases: a non-detection is weak evidence.
4. Stellar confusion. The host star (especially an M dwarf) produces ECM and plasma bursts with the same signatures.
5. Uncertain theory. Field scaling laws, the radiometric Bode's law, and wind models each carry order-of-magnitude uncertainty.

Low-frequency instrumental issues (ionosphere, RFI, sidelobes of bright sources) add false positives: beam-formed data are especially vulnerable.

Has exoplanet radio emission been detected?

Not yet, securely

No exoplanet has a confirmed radio detection. Candidates are *star–planet interaction*: emission from the star, at the star's ν_c, possibly tied to a planet's orbit.

Target	Claim	Instrument	Status
GJ 1151	120–167 MHz, polarized, quiescent M dwarf	LOFAR (Vedantham et al. 2020)	uGMRT: no detection (Narang et al. 2024); emission variable
YZ Ceti	coherent bursts near the inner planet's phase	VLA 2–4 GHz (Pineda & Villadsen 2023); uGMRT (Trigilio et al. 2023)	suggestive; stellar activity not excluded
τ Boötis b	tentative low-frequency burst	LOFAR (Turner et al. 2021)	not confirmed

Pineda & Villadsen 2023, doi:10.1038/s41550-023-01914-0; Trigilio et al. 2023, arXiv:2305.00809; Narang et al. 2024, arXiv:2409.18507. Other references: next slides.

Star–planet interaction: emission from the star

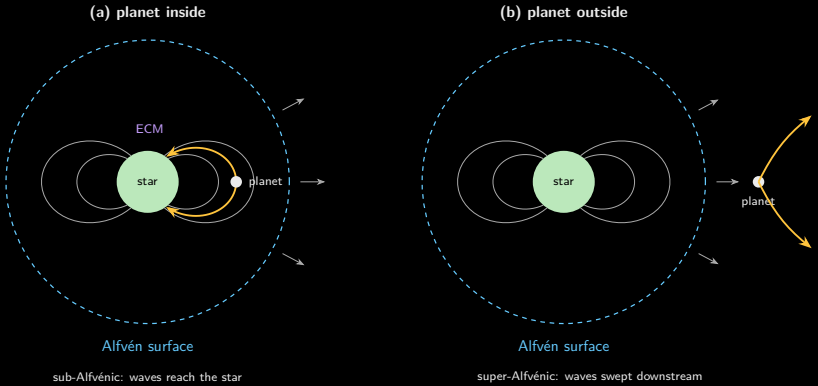
- A planet orbiting inside the star's Alfvén surface (sub-Alfvénic flow) can drive currents along stellar field lines, as Io does at Jupiter.
- The emission is then generated in the *star's* magnetosphere, at the *stellar* ν_c.
- Signature: modulation at the *orbital* (or synodic) period, not the stellar rotation period.

LOFAR M-dwarf population

Many nearby M dwarfs show circularly polarized 144 MHz emission [Callingham et al. 2021, doi:10.1038/s41550-021-01483-0]. Some are magnetically quiescent stars, motivating star–planet interaction as one explanation.

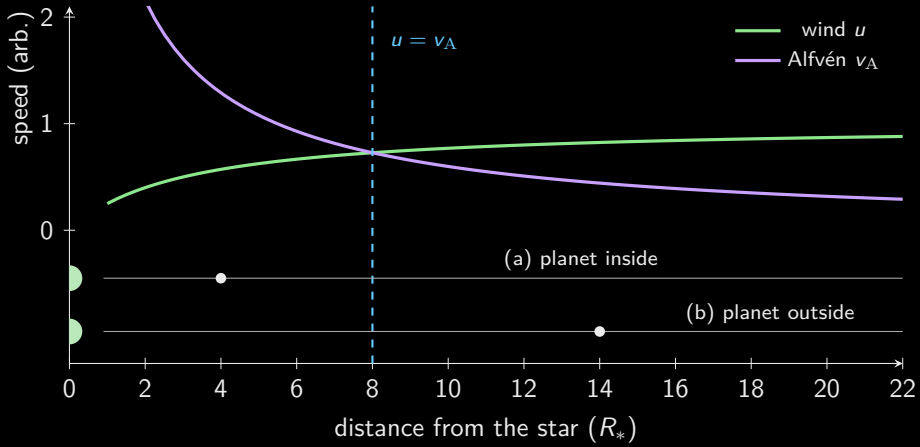
Requires an independent planet detection and phase-locked repeatability.

Why the planet must lie inside the Alfvén surface



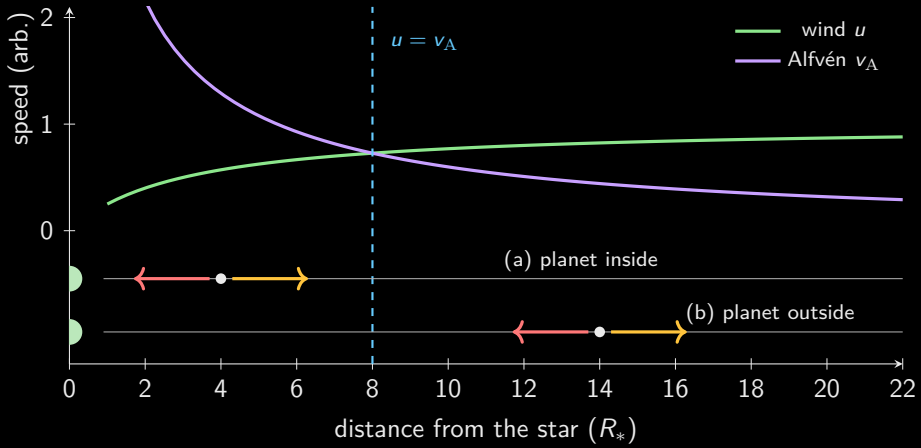
- Inside: the planet–field disturbance travels upstream along the field as an Alfvén wave; electrons accelerated near the star emit ECM at the stellar ν_c.
- Outside: the wind outruns the waves.

Alfvén waves from a planet



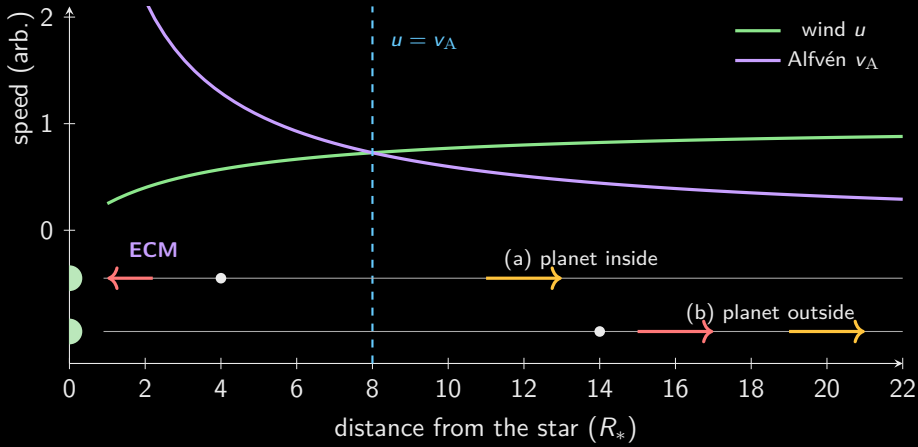
- Waves move along the field at $u \pm v_A$ (outward, $\rightarrow$; inward, $\leftarrow$).
- Planet (a) is where $v_A > u$; planet (b) is where $u > v_A$.

Alfvén waves from a planet



- Waves move along the field at $u \pm v_A$ (outward, $\rightarrow$; inward, $\leftarrow$).
- Both planets launch a packet each way.

Alfvén waves from a planet



- Waves move along the field at $u \pm v_A$ (outward, $\rightarrow$; inward, $\leftarrow$).
- (a) the inward packet reaches the star; (b) both packets are swept outward

Case comparison: grade the strength of each inference

Case	Observed	Inferred	Strength
Jupiter	resolved sources, in-situ spacecraft, Io phase, rotation period	ECM in auroral cavities; $B \approx 14\,\mathrm{G}$ at footprints	secure
Active M dwarf flare	100% circular, narrow band, $T_\mathrm{b} \gg 10^{10}\,\mathrm{K}$	coherent (ECM or plasma); local B or n_e	mechanism good; location weak
GJ 1151	circularly polarized 120–167 MHz emission from a quiescent M dwarf	star–planet interaction proposed	suggestive; companion not confirmed
τ Boötis b	tentative 14–21 MHz burst in beam-formed data	planetary ECM	not confirmed interferometrically

GJ 1151: Vedantham et al. 2020, doi:10.1038/s41550-020-1011-9; Pope et al. 2020 (no massive companion), doi:10.3847/2041-8213/ab5b99. τ Boo: Turner et al. 2021, doi:10.1051/0004-6361/201937201; Cordun et al. 2025 (interferometric upper limit), doi:10.1051/0004-6361/202452868.

Robust signatures and common false positives

Robust positive signatures

- Repetition locked to the *orbital* phase over many cycles
- Same polarization sense at the same phase
- Spectral cutoff consistent across epochs
- Localization by imaging (direction of arrival)

Common false positives

- Stellar flares (plasma or ECM) from the host
- RFI and ionospheric scintillation
- Off-axis bright sources leaking into beam-formed data
- Few-epoch “periodicity” from sparse sampling

Concept test

Question

Circularly polarized low-frequency bursts from an M dwarf recur with a 2.6-day period. The star rotates once in 30 days; a candidate planet orbits in 2.6 days. Which interpretation does the period favour, and what would secure it?

Concept test

Question

Circularly polarized low-frequency bursts from an M dwarf recur with a 2.6-day period. The star rotates once in 30 days; a candidate planet orbits in 2.6 days. Which interpretation does the period favour, and what would secure it?

Answer: star–planet interaction; secure it with an independent planet detection and phase-locked repetition

1. Emission from the star's own magnetosphere is modulated at the *rotation* period; modulation at the *orbital* period points to currents driven by the planet, as Io does at Jupiter.
2. A few bursts can mimic a period; repetition locked to orbital phase over many cycles, plus a planet found by another method, makes the case.

Retrieval: is this H II region optically thin?

Two continuum measurements

An unresolved H II region has $S_{1.4\,\mathrm{GHz}} = 0.50\,\mathrm{Jy}$ and $S_{5\,\mathrm{GHz}} = 0.90\,\mathrm{Jy}$. Is it optically thin at 1.4 GHz?

Retrieval: is this H II region optically thin?

Two continuum measurements

An unresolved H II region has $S_{1.4\,\mathrm{GHz}} = 0.50\,\mathrm{Jy}$ and $S_{5\,\mathrm{GHz}} = 0.90\,\mathrm{Jy}$. Is it optically thin at 1.4 GHz?

$$\alpha = \frac{\ln(0.90/0.50)}{\ln(5/1.4)} = \frac{0.588}{1.273} \approx +0.46$$

- Optically thin free-free gives $\alpha \approx -0.1$; fully thick gives $\alpha = +2$.
- $+0.46$ lies between: the source is partially optically thick at 1.4 GHz (and possibly at 5 GHz), or is a blend of components with different EM.
- Only a third, higher frequency shows where the spectrum turns over.

Retrieval: is this H II region optically thin?

Two continuum measurements

An unresolved H II region has $S_{1.4\,\mathrm{GHz}} = 0.50\,\mathrm{Jy}$ and $S_{5\,\mathrm{GHz}} = 0.90\,\mathrm{Jy}$. Is it optically thin at 1.4 GHz?

$$\alpha = \frac{\ln(0.90/0.50)}{\ln(5/1.4)} = \frac{0.588}{1.273} \approx +0.46$$

- Optically thin free-free gives $\alpha \approx -0.1$; fully thick gives $\alpha = +2$.
- $+0.46$ lies between: the source is partially optically thick at 1.4 GHz (and possibly at 5 GHz), or is a blend of components with different EM.
- Only a third, higher frequency shows where the spectrum turns over.

Central question

How do continuum and recombination-line observations reveal embedded ionized structures?

Why radio for H II regions?

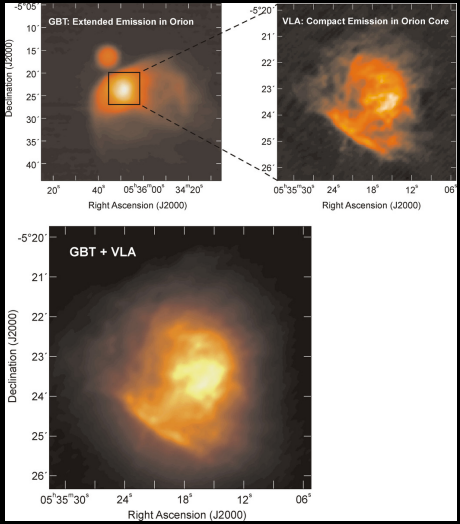
- Massive stars form deep inside molecular clouds: A_V of tens to hundreds of magnitudes. Hα is invisible.
- Radio free-free emission and radio recombination lines (RRLs) pass through dust unattenuated.
- Both arise from the same ionized gas, so they measure the *ionizing output* of the embedded stars.

Two radio tracers

- Continuum: EM, n_e, size, Q_Lyc
- RRLs: velocity (hence distance), T_e, $\mathrm{He}^+/\mathrm{H}^+$

Units: cgs for emissivities and recombination coefficients; EM in $\mathrm{pc\,cm^{-6}}$; fluxes in Jy.

The Orion Nebula: single-dish and interferometer views



Credit: 3.6 cm continuum of the Orion Nebula: GBT (extended), VLA (compact core), and combined. NRAO/AUI, CC BY 3.0, Wikimedia Commons (from images.nrao.edu)

Ionization balance: the Strömgren sphere (review)

Assumptions: one star emitting Q hydrogen-ionizing photons per second into uniform pure hydrogen of density n; full ionization inside $R_{\rm S}$; "on-the-spot" Case B recombination; no dust; steady state.

$$Q = \frac{4\pi}{3} R_{\rm S}^3 \, n_{\rm e} n_{\rm p} \, \alpha_{\rm B} \quad \Rightarrow \quad R_{\rm S} = \left(\frac{3Q}{4\pi n^2 \alpha_{\rm B}} \right)^{1/3}$$

with $\alpha_{\rm B} \approx 2.6 \times 10^{-13} \, {\rm cm^3 \, s^{-1}}$ at $T_{\rm e} = 10^4$ K.

n (cm^{-3}), $Q = 10^{49}$ s^{-1}	10^2	10^3	10^4	10^5
$R_{\rm S}$ (pc)	3.1	0.68	0.15	0.03

$R_{\rm S} \propto n^{-2/3}$: the same star makes a small, dense, bright H II region in dense gas.

Where the ideal model fails

- Density gradients: real clouds are centrally concentrated; the ionization front can break out on one side.
- Clumping: filling factor $f < 1$; n_e from EM is an rms value (L4).
- Dust inside the ionized gas absorbs part of Q.
- Leakage: ionizing photons escape through holes.
- Clusters: several stars, not one.

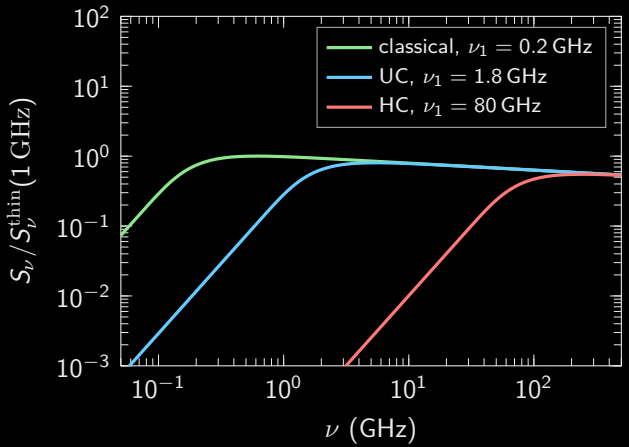
Expansion

Ionized gas at $T_\mathrm{e} \sim 10^4\,\mathrm{K}$ is overpressured relative to its ~ 10–$100\,\mathrm{K}$ surroundings by $\sim 10^2$–10^3. It expands at about the ionized sound speed $c_\mathrm{i} \approx 10\,\mathrm{km\,s^{-1}}$ behind a shock (Spitzer solution):

$$R(t) = R_\mathrm{S}\left(1 + \frac{7 c_\mathrm{i} t}{4 R_\mathrm{S}}\right)^{4/7}.$$

Approximate; uniform medium [Spitzer, *Physical Processes in the Interstellar Medium*, 1978].

Free-free spectra shift to higher frequency as regions get denser

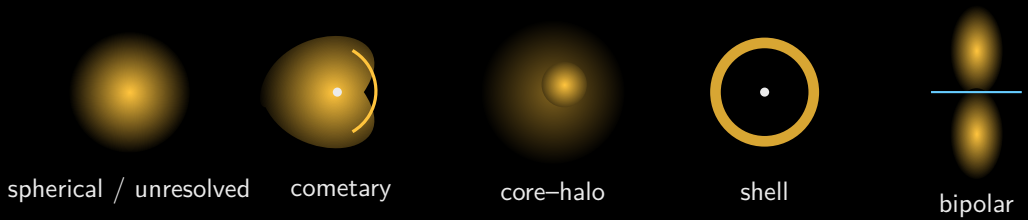


$$S_\nu \propto \nu^2 \left(1 - \mathrm{e}^{-\tau_\nu}\right)$$

$$\tau_\nu = (\nu/\nu_1)^{-2.1}$$

- Uniform slabs, same thin flux at high ν (schematic).
- Observed HC regions often show $\alpha \approx +1$ over a wide range: density gradients.

UC H II morphologies



Schematic; classes after Wood & Churchwell (1989) and Churchwell (2002), doi:10.1146/annurev.astro.40.060401.093845.

- Cometary: bright arc facing a density peak or the direction of stellar motion. Models: bow shock (moving star) or champagne flow (ionized gas escaping down a density gradient). RRL velocity gradients along the tail discriminate them.
- Shell: wind-blown cavity. Bipolar: ionized gas escaping perpendicular to a dense disc or torus.

Concept test

Question

Two H II regions have the same optically thin flux density at high frequency. One turns over near 0.2 GHz, the other near 80 GHz. Which is the denser, and which would a 1.4 GHz survey underestimate?

Concept test

Question

Two H II regions have the same optically thin flux density at high frequency. One turns over near 0.2 GHz, the other near 80 GHz. Which is the denser, and which would a 1.4 GHz survey underestimate?

Answer: the 80 GHz one, on both counts

1. $\tau_\nu \propto \mathrm{EM}\,\nu^{-2.1}$, so a higher turnover frequency needs a larger EM: a denser, more compact (hypercompact) region.
2. Below its turnover the flux falls as ν^2, so at 1.4 GHz the hypercompact region is thick and far fainter than its thin flux.

Radio recombination lines

Hydrogen $n+1 \to n$ (α) transitions, from the Rydberg formula:

$$\nu_{n\alpha} = R_{\rm H} c \left[\frac{1}{n^2} - \frac{1}{(n+1)^2}\right] \approx \frac{2 R_{\rm H} c}{n^3} \approx \frac{6.58\,{\rm GHz}}{(n/100)^3}$$

Line	H166α	H110α	H109α	H91α
ν (GHz)	1.424	4.874	5.009	8.584

- Reduced-mass shifts: He and C lines appear at -122 and $-150\,{\rm km\,s^{-1}}$ relative to H at the same n. One spectrum gives H^+, He^+, and (from PDRs) C^+.
- Thermal width of H at 10^4 K: $\Delta v_{\rm FWHM} = (8 \ln 2\, k_{\rm B} T_{\rm e}/m_{\rm H})^{1/2} \approx 21\,{\rm km\,s^{-1}}$. Observed widths $\sim$ 20–30 $\,{\rm km\,s^{-1}}$ include turbulence and flows.

Recombination lines with the GMRT

- Low frequencies suit RRLs from carbon in cold gas: the lines are strongest below ~ 1 GHz and narrow, and many n fall in one band.
- The wide band lets one observation cover many lines (e.g. Cα 244–250) and stack them in the visibility domain.
- GMRT baselines map the line gas at sub-parsec resolution.

Results

- Cas A carbon lines resolved into clumps tracing a PDR-like layer in the Perseus arm: Chowdhury & Chengalur 2019, doi:10.1093/mnras/stz779.
- Hydrogen lines at 0.6 and 1.28 GHz from a shell H II region at $l = 24.8°$: Kantharia et al. 2007, doi:10.1007/s12036-007-0005-7.

Electron temperature from the line-to-continuum ratio

Assumptions: LTE level populations, optically thin line and continuum, Gaussian line, same gas emits both.

1. Continuum: $\tau_{\mathrm{C}} \propto \mathrm{EM}\, T_{\mathrm{e}}^{-1.35} \nu^{-2.1}$ (L4).
2. Line peak (LTE): $\tau_{\mathrm{L}} \propto \mathrm{EM}\, T_{\mathrm{e}}^{-2.5}\, \nu^{-1}\, \Delta v^{-1}$ (higher T_{e} depopulates bound levels and widens the line).
3. Ratio: EM *cancels*, leaving $T_{\mathrm{L}}/T_{\mathrm{C}} \propto \nu^{1.1}\, T_{\mathrm{e}}^{-1.15} \Delta v^{-1}$.

$$T_{\mathrm{e}}^{*} \approx \left[\frac{6985}{a(\nu, T_{\mathrm{e}})} \left(\frac{\nu}{\mathrm{GHz}} \right)^{1.1} \frac{T_{\mathrm{C}}}{T_{\mathrm{L}}} \left(\frac{\Delta v}{\mathrm{km\,s^{-1}}} \right)^{-1} \frac{1}{1 + y^{+}} \right]^{0.87} \mathrm{K}$$

- $a \approx 1$ is a Gaunt-factor correction; $y^{+} = n(\mathrm{He}^{+})/n(\mathrm{H}^{+})$. TRA Ch. 14 (approximate formula).
- Caveats: non-LTE (stimulated emission), pressure broadening at high n_{e} and n, and blended velocity components.

Worked example: an RRL electron temperature

H109α at $\nu = 5.009\,\mathrm{GHz}$ (illustrative values): $T_\mathrm{L}/T_\mathrm{C} = 0.050$, $\Delta v = 25\,\mathrm{km\,s^{-1}}$, $y^+ = 0.08$, $a = 1$.

$$T_\mathrm{e}^* = \left[6985 \times 5.009^{1.1} \times \frac{1}{0.050} \times \frac{1}{25} \times \frac{1}{1.08}\right]^{0.87}$$
$$= \left[6985 \times 5.88 \times 20 \times 0.040 \times 0.926\right]^{0.87} = \left(3.04 \times 10^4\right)^{0.87} \approx 7.9 \times 10^3\,\mathrm{K}$$

Worked example: an RRL electron temperature

H109α at $\nu = 5.009\,\mathrm{GHz}$ (illustrative values): $T_\mathrm{L}/T_\mathrm{C} = 0.050$, $\Delta v = 25\,\mathrm{km\,s^{-1}}$, $y^+ = 0.08$, $a = 1$.

$$T_\mathrm{e}^* = \left[6985 \times 5.009^{1.1} \times \frac{1}{0.050} \times \frac{1}{25} \times \frac{1}{1.08}\right]^{0.87}$$
$$= [6985 \times 5.88 \times 20 \times 0.040 \times 0.926]^{0.87} = (3.04 \times 10^4)^{0.87} \approx 7.9 \times 10^3\,\mathrm{K}$$

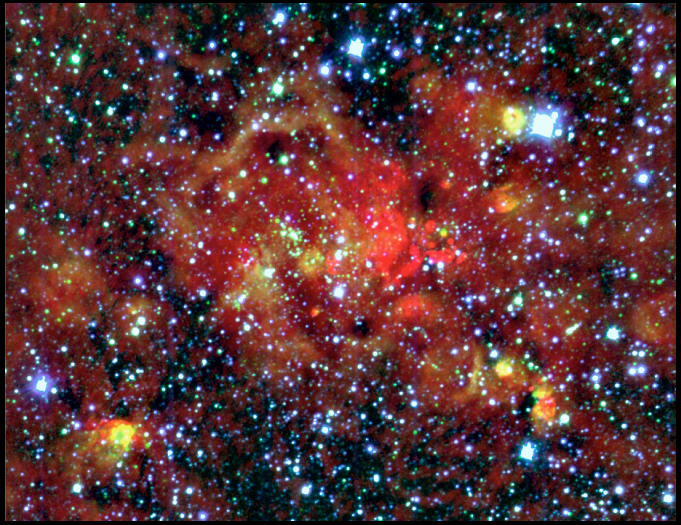
- Sensitivity: $T_\mathrm{e} \propto (T_\mathrm{L}/T_\mathrm{C})^{-0.87}$. A 20% error in the ratio gives a $\approx 17\%$ error in T_e.
- Galactic H II regions show T_e rising with Galactocentric radius: fewer metals, less cooling. RRL T_e is a radio metallicity proxy [Balser et al. 2011, doi:10.1088/0004-637X/738/1/27].

What continuum and lines give, together

Quantity	From	Requires
EM, turnover ν_1	continuum spectrum	T_e (weakly)
rms n_e	EM + angular size	distance, path length, f
Q_Lyc	thin continuum flux	distance, T_e, no dust or leakage
T_e	RRL/continuum ratio	LTE, thin, unblended
$\mathrm{He}^+/\mathrm{H}^+$	He and H RRLs	both ionized zones sampled

- None of these uses optical or near-IR light: an extinction-free census of massive-star formation.
- Surveys combine RRLs with mid-IR to catalogue Galactic H II regions [Anderson et al. 2014, doi:10.1088/0067-0049/212/1/1].

W49A: embedded ionized gas



Credit: W49A: 3.6 cm radio continuum (red) with ESO NTT/SofI K_s (green) and J (blue). ESO, CC BY 4.0, eso0322b. Red-only features: ionized gas too embedded to be seen in the near-IR

Interpreting a complex star-forming region

Several components in one field (illustrative):

Comp.	$\alpha_{1.4}^{5}$	Pol.	RRL
A	$+1.6$	0	broad
B	-0.1	0	yes
C	-0.7	12%	no
D	-0.3	0	weak

- Classify each component, then write the evidence.

Interpreting a complex star-forming region

Several components in one field (illustrative):

Comp.	$\alpha_{1.4}^{5}$	Pol.	RRL
A	$+1.6$	0	broad
B	-0.1	0	yes
C	-0.7	12%	no
D	-0.3	0	weak

- Classify each component, then write the evidence.

- A: thick, dense: UC/HC H II candidate (or a thermal jet).
- B: thin thermal H II region.
- C: non-thermal: SNR, background radio galaxy, or colliding-wind binary.
- D: blend: e.g. equal thermal and $\alpha = -0.8$ components give $\alpha \approx -0.37$ between 1.4 and 5 GHz.

Test D: map α at matched resolution; RRL-predicted thermal flux.

Summary and further reading

- Ultracool dwarfs: coherent auroral (ECM) radio emission is detected; for exoplanets, detection is still unconfirmed, and star–planet interaction inside the Alfvén surface is the most promising route.
- H II regions: free-free continuum and RRLs trace the same ionized gas, free of dust extinction. The Strömgren balance links Q, n and size; density sets the turnover frequency.
- RRLs give velocity and $T_{\rm e}$ (from $T_{\rm L}/T_{\rm C}$, independent of EM); the GMRT detects them at low frequency.

Further reading

Vedantham et al. 2020 (GJ 1151); Pineda & Villadsen 2023 (YZ Ceti); Chowdhury & Chengalur 2019 (GMRT RRLs); ERA Ch. 4 and Ch. 7; TRA Ch. 11 and Ch. 14.

Next lecture

Synchrotron contamination, ionizing photons, SNRs, PWNe and the Galactic Centre.